Molecular Cell, Volume *30*

Supplemental Data

The CUL7 E3 Ubiquitin Ligase

Targets Insulin Receptor Substrate 1

for Ubiquitin-Dependent Degradation

Xinsong Xu, Antonio Sarikas, Dora C. Dias-Santagata, Georgia Dolios, Pascal J. Lafontant, Shih-Chong Tsai, Wuqiang Zhu, Hidehiro Nakajima, Hisako O. Nakajima, Loren J. Field, Rong Wang, and Zhen-Qiang Pan

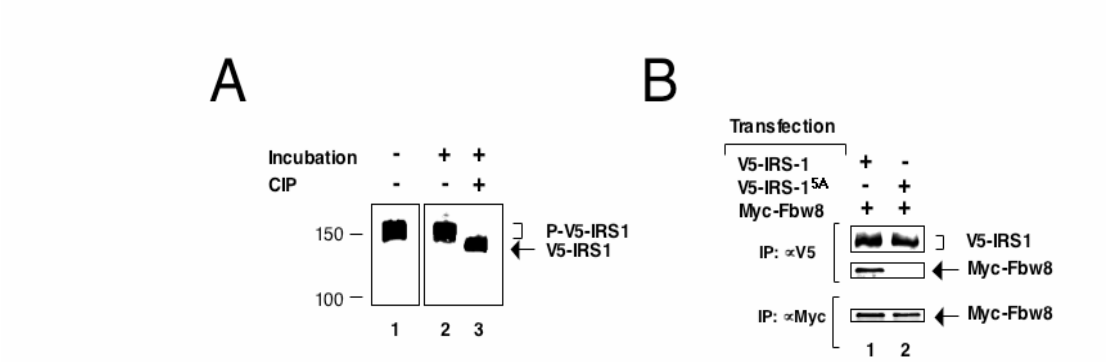

Supporting Fig.1
Xu et al.

Figure S1.

Analysis of ectopically expressed IRS-1 in HEK293 cells. A) V5-IRS-1 is extensively phosphorylated. We examined the phosphorylation status of V5-IRS-1 expressed in HEK293 cells. For this purpose, extracts of HEK293 cells containing over-expressed V5-IRS-1 (25μg of protein) were diluted 20-fold with CIP de-phosphorylation buffer, followed by incubation (lanes 2 and 3), or not (lane 1), at 37°C for 30min in the absence

(lane 2) or presence of CIP (10 unit; lane 3). One third of the reaction mixture was electrophoresed through 6% SDS-PAGE and probed for V5. The results showed that all forms of V5-IRS-1 were converted into a fast-migrating species upon incubation with alkaline phosphatase. Similar results were observed with λ-phosphatase (data not shown). Thus, V5-IRS-1, when expressed in HEK293 cells, is phosphorylated extensively. **B) Mutation 5A reduces IRS-1' ability to interact with Fbw8.** Co-immunoprecipitation experiments were employed to evaluate the effects of quintuple mutation (5A) on interactions with Fbw8. Note that adjustment was made in this assay in order to express V5-IRS-1 at levels high enough to evaluate interactions with Myc-Fbw8. For this purpose, high amount of vector DNA for V5-IRS-1 or mutant 5A (2μg of DNA instead of 1μg in the other experiments) was introduced into HEK293 cells. As shown, while the wild type V5-IRS-1 interacted with Myc-Fbw8 in HEK293 cells, the association between Myc-Fbw8 and V5-IRS-1^{5A} was barely detectable (compare lanes 1 and 2), despite the presence of comparable amounts of Myc-Fbw8 and V5-IRS-1 or mutant 5A. Thus, it is likely that the quintuple mutation (5A) impairs IRS-1's ability to interact with Fbw8.

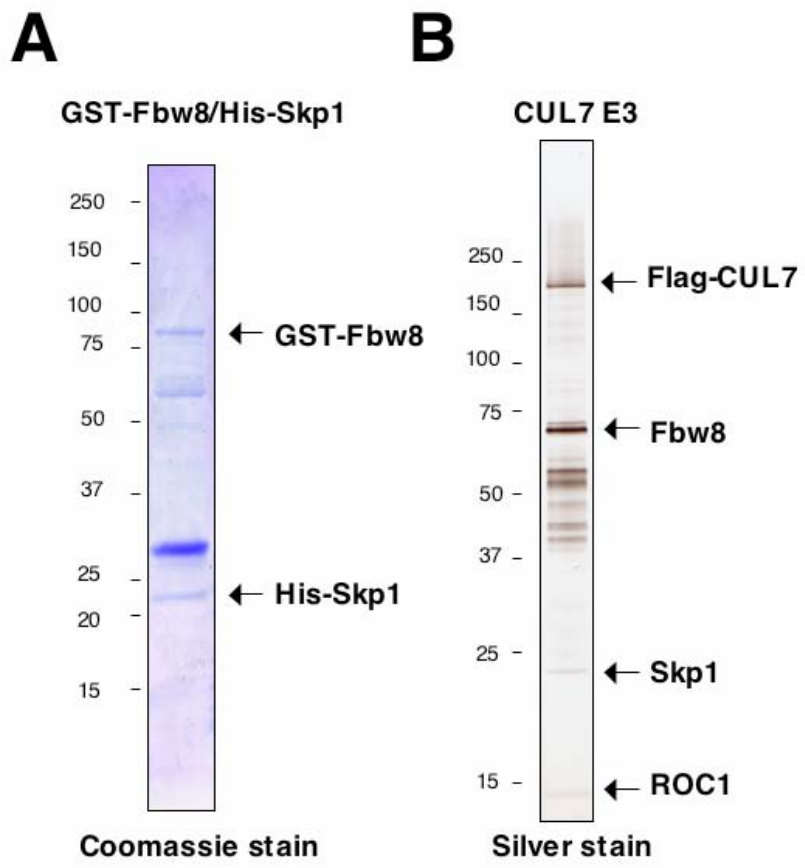

Supporting Fig.2
Xu et al.

Figure S2.

A) Coomassie stain analysis of GST-Fbw8/His-Skp1. A complex of GST-Fbw8 and Skp1 was assembled in bacteria (BL21) transformed with pGEX-4T3/pET-15b-(GST-Fbw8)-(His-Skp1). Typically, extracts (200µl), prepared as previously described (Wu *et al*., 2000b), were absorbed to glutathione beads (20µl) and the resulting matrix was washed extensively and used for binding experiment. It is estimated that the beads contained approximately 1µg of the GST-Fbw8/Skp1 complex. Glutathione beads (20µl)

coupled with 5µg of GST were used as control. Shown is Coomassie stain analysis of purified GST-Fbw8/Skp1 complex (~0.5µg). **B) Silver stain analysis of the affinity-purified CUL7 E3.** Twenty five liters of 293FC7 cells that constitutively express Flag-CUL7 were grown in suspension, and extracts (20ml) were prepared and adsorbed to M2 matrix (0.5ml), followed by elution of the CUL7 E3 with Flag peptide, using procedures described previously (Dias *et al*., 2002). The elutes were concentrated to a final volume of 100µl (~0.5pmol/µl) by using centrifugal filters (Millipore). An aliquot (0.3pmol) was analyzed by 4-20% SDS-PAGE followed by silver stain.

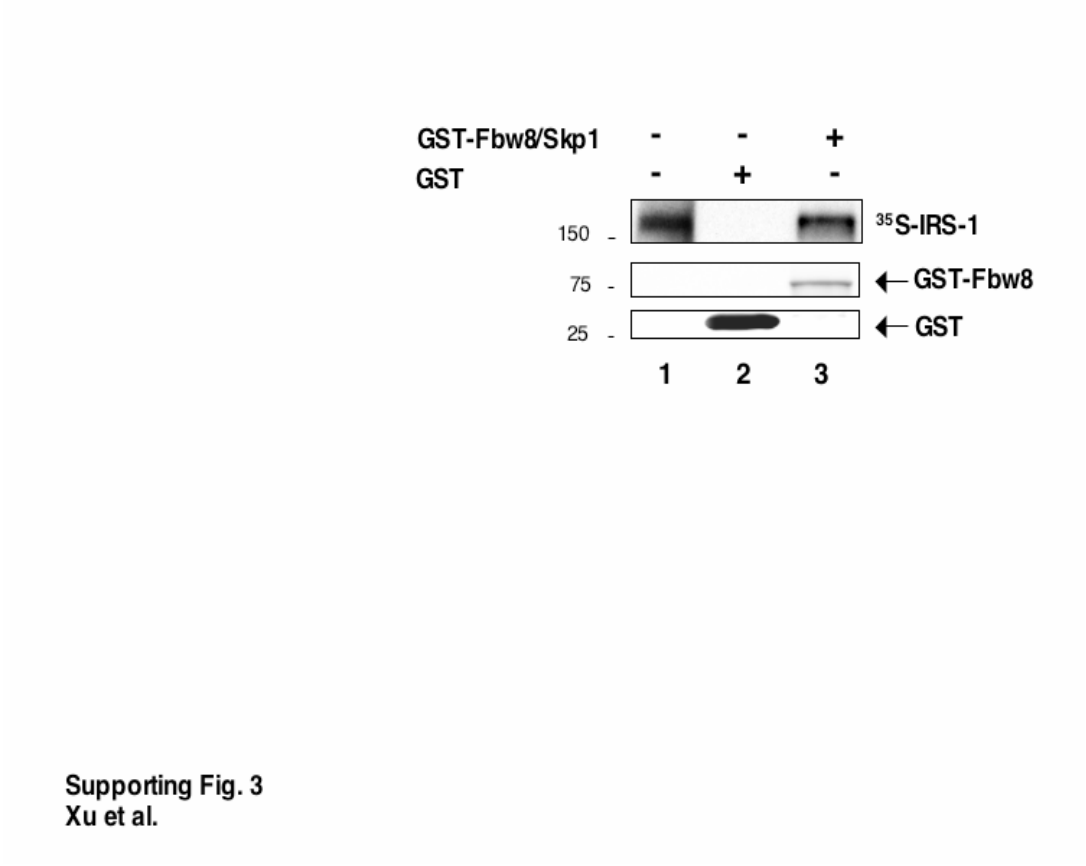

Figure S3.

^{35}S-IRS-1 is bound to GST-Fbw8/Skp1. Glutathione beads (20μl), containing approximately 1μg of the GST-Fbw8/Skp1 complex or 5μg of GST, were prepared as described in supporting Fig. 2A. The beads were mixed with ^{35}S-IRS-1 (5μl), synthesized from the rabbit reticulolysates (TNT Coupled Reticulocyte Lysate Systems, Promega Corp.). The mixture was incubated at 4°C for 1h on a thermomixer (1,300rpm; Eppendorf) and the resulting beads were washed 3 times with buffer containing 10mM Tris-HCl, pH 7.4, 500mM NaCl, 0.5%NP-40, 5mM EDTA, and 5mM EGTA, prior to separation through 6% SDS-PAGE analysis followed by autoradiography. Input ^{35}S-IRS-1 (20%) was shown in lane 1.

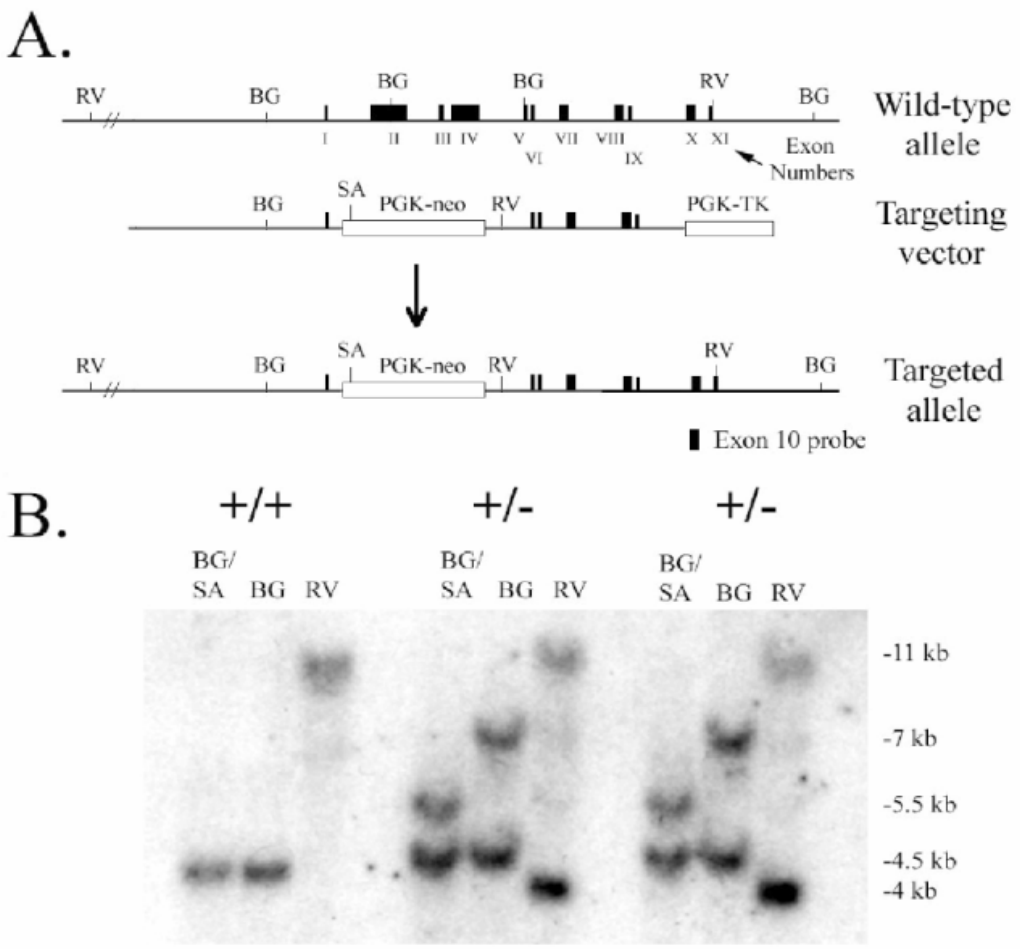

Supporting Fig. 4
Xu et al.

Figure S4.

Genetic ablation of mouse *cul7*. A) A diagram for *cul7* targeting strategy. The mouse CUL7 locus was disrupted by homologous recombination. The CUL7 gene spans ca. 14.2 kb of genomic DNA, and consists of 26 exons. The targeting vector spanned ca. 10 kb of CUL7 genomic DNA encompassing 4 kb of 5′ flanking sequence through intron 9. Within the targeting vector, exons 2-4 were replaced with a PGK-neo cassette such that the CUL7 translation initiation site (located in exon 2) would be disrupted via homologous recombination. A PGK-TK cassette was inserted into the 3′ end of the

targeting vector. The DNA was linearized and electroporated into CCE ES cells using standard techniques. G418-resistant/gancyclovir resistant clones were isolated and screened via Southern blot to identify correctly targeted homologous recombination events. Digestion of the wild-type CUL7 allele with Bgl II + Sal I (BG+SA), Bgl II (BG), and Eco RV (RV) gives rise to restriction fragments of 4.5, 4.5 and 11 kb, respectively, when hybridized with an exon 10 probe (note that exon 10 lies outside of the targeting vector). Digestion of a correctly targeted CUL7 allele with Bgl II + Sal I, Bgl II, and Eco RV gives rise to restriction fragments of 5.5, 7 and 4 kb, respectively, when hybridized with an exon 10 probe. **B) Southern analysis.** A diagnostic Southern blot of DNA from one wild type and two targeted ES clones is shown. The pattern of the restriction digests indicates that the two clones were correctly targeted.

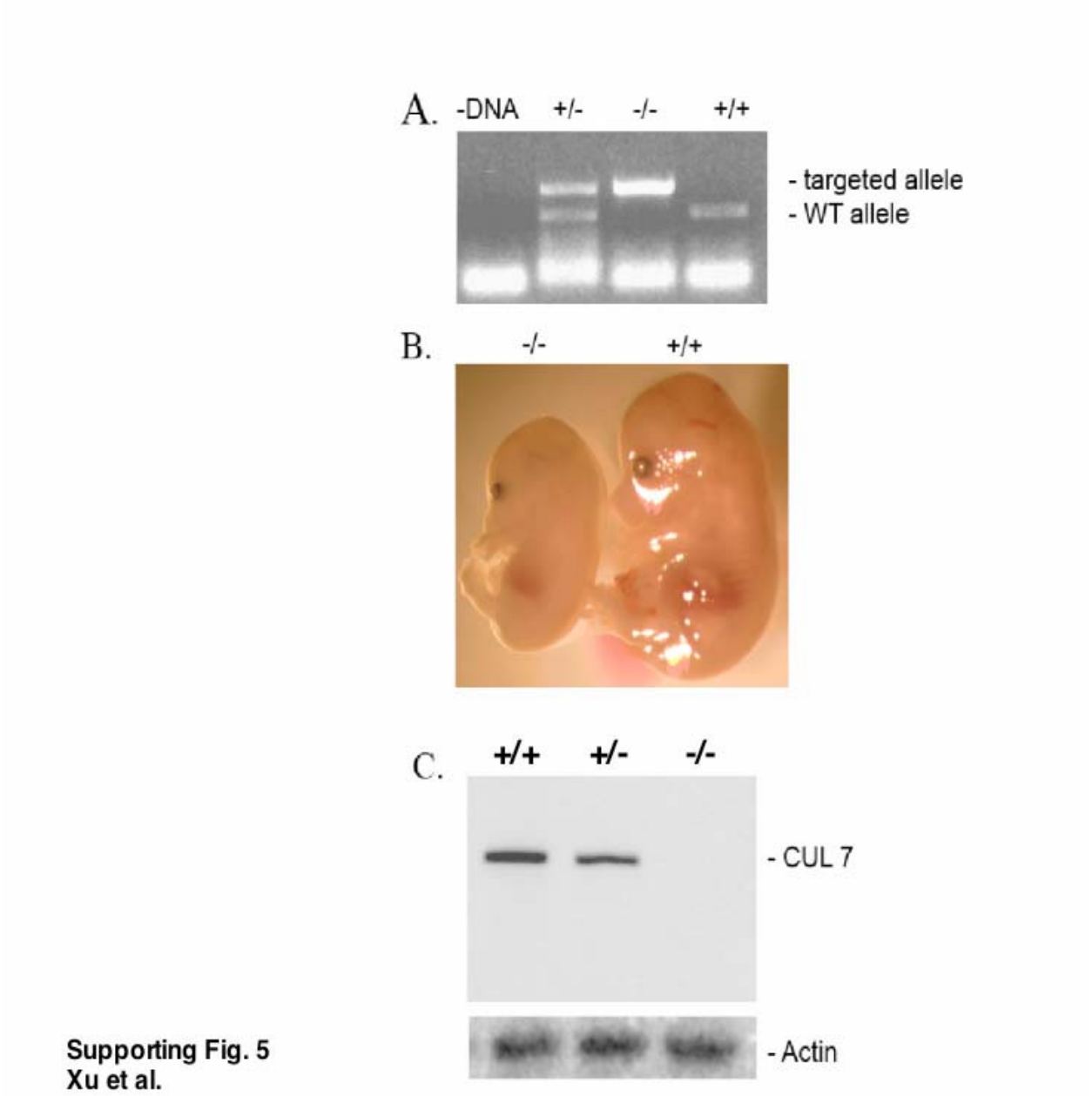

Figure S5.

Generation and analysis of *cul7*$^{-/-}$ mice. A) Genotyping *cul7*$^{-/-}$ mice. Three targeted ES cell lines were generated and injected into recipient C57Bl/6J blastocysts. The chimeric animals produced from these crosses were bred, and germ line transmission was observed with chimeras from two of the ES cell lines. CUL7$^{+/-}$ mice were then

interbred; no homozygous CUL7$^{-/-}$ offspring were observed (a total of 114 offspring mice were screened; 33 CUL7 +/+ and 77 CUL7$^{+/-}$ were obtained), suggesting that loss of CUL7 might result in embryonic lethality. Accordingly, timed pregnancies were generated, and embryos were harvested at 14.5 days PC. A diagnostic PCR assay was used to genotype the embryos. Embryos with CUL7$^{-/-}$ genotype were readily identified. **B) Growth defects of *cul7*$^{-/-}$ mice.** CUL7$^{-/-}$ littermates exhibited gross growth retarded as compared to CUL7$^{+/+}$. This phenotype is very similar to that observed by DeCaprio and colleagues (Arai *et al.*, 2003). **C) Immunoblot analysis of CUL7$^{+/+}$ and CUL7$^{-/-}$ MEFs.** Western blot analyses with a CUL7-specific monoclonal antibody (Dowell *et al.*, 2007) revealed an approximately 50% reduction in CUL7 protein levels in embryonic fibroblasts isolated from CUL7$^{+/-}$ embryos as compared to fibroblasts from CUL7$^{+/+}$. No CUL7 protein was detected in embryos from CUL7$^{-/-}$ embryos. The lower panel shows the load control (actin was visualized).

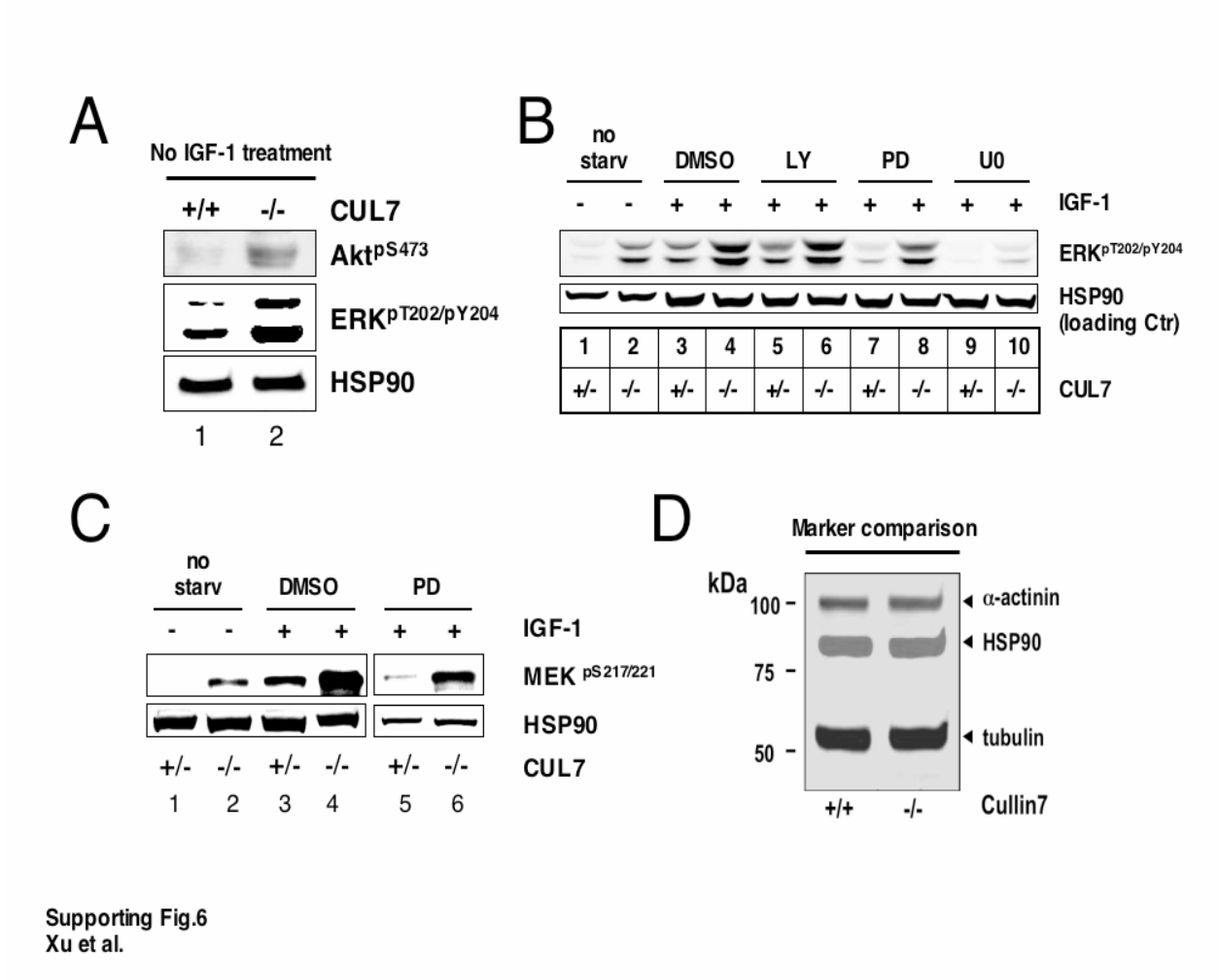

Supporting Fig.6
Xu et al.

Figure S6.

Analysis of Akt and ERK signaling in *Cul7*$^{-/-}$ MEFs. A) Activation of Akt and ERK in *Cul7*$^{-/-}$ MEFs. MEFs were grown in DMEM plus 10% FBS. Extracts (50μg of protein) were separated by 10% SDS-PAGE followed by immunoblot analysis to monitor the levels of activated Akt and ERK. **B) Effects of PI3-K and MEK inhibitors on ERK signaling in *Cul7*$^{-/-}$ MEFs.** MEFs were serum-starved for 16h prior to treatment with IGF-1 (3nM) for 30min. For inhibitor experiments, cells were treated with PD98059 (50μM), U0126 (10μM), or LY294002 (50μM) one hour prior to the addition of IGF-1 and these inhibitors remained in the culture media for the duration of IGF-1 treatment.

Extracts (100μg of protein) were separated by 10% SDS-PAGE followed by immunoblot analysis to monitor the levels of activated ERK. In lanes 1 and 2, cells were not serum starved. Note that *Cul7*$^{+/-}$ and *Cul7*$^{+/+}$ MEFs were nearly identical in response to IGF-1 for activation of ERK. **C) Effects of PD98059 on MEK activity.** MEFs were treated without (lanes 1 and 2) or with (lanes 3-6) serum-starvation for 16h. Cells were then treated with DMSO (lanes 3 and 4) PD98059 (50μM; lanes 5 and 6) one hour prior to the addition of IGF-1 (3nM) and the inhibitor remained in the culture media for the duration of IGF-1 treatment (30min). Extracts (100μg of protein) were separated by 10% SDS-PAGE followed by immunoblot analysis to monitor the levels of activated MEK (MEK$^{pS217/221}$). Of note, *Cul7*$^{+/-}$ and *Cul7*$^{+/+}$ MEFs are nearly identical in response to IGF-1 for activation of MEK. **D) Comparison of various markers for loading control.** Extracts (100μg of protein) from *Cul7*$^{+/+}$ and *Cul7*$^{-/-}$ MEFs were compared for various loading markers.

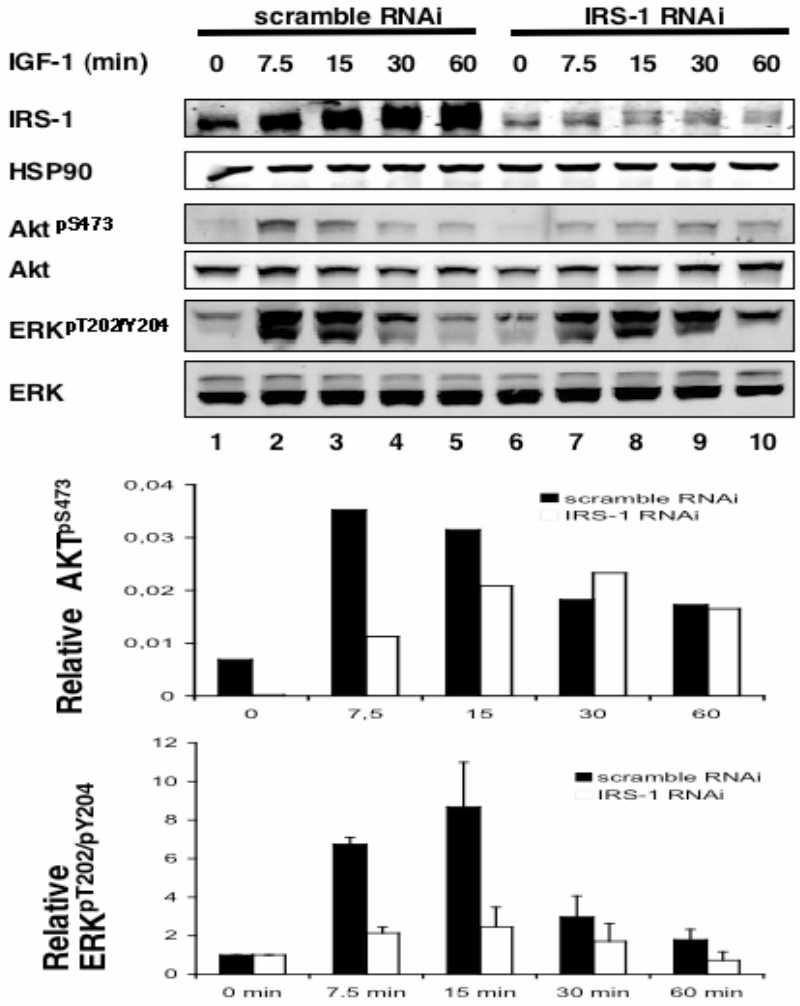

Supporting Fig.7
Xu et al.

Figure S7.

IRS-1 depletion decreases Akt and ERK activation in response to IGF-1. CUL7$^{-/-}$ MEFs (at passage 4) were treated with scramble siRNA (lanes 1-5) or IRS-1 siRNA (lanes 6-10)

at a concentration of 24nM. SiRNA was obtained from Dharmacon and transfection was carried out following Dharmacon's instruction. At 32h post-transfection, the MEFs were serum-starved for 16h prior to treatment with (lanes 2-5 and 7-10) or without (lanes 1 and 6) IGF-1 (3nM) for indicated times. Extracts (50μg of protein) were separated by 6% or 4-20% SDS-PAGE followed by immunoblot analysis to monitor the levels of IRS-1, phosphorylated and total Akt and ERK, as well as HSP90 (as a control for equal loading). The relative amounts of phosphorylated and total Akt or ERK were quantitated by Odyssey Infrared Imaging and the ratio of phosphorylated Akt (or ERK) *vs* total pool is expressed graphically. While the Akt graph depicts the quantitation of the representative blot shown in this figure, the ERK graph summarizes the results of two independent experiments.

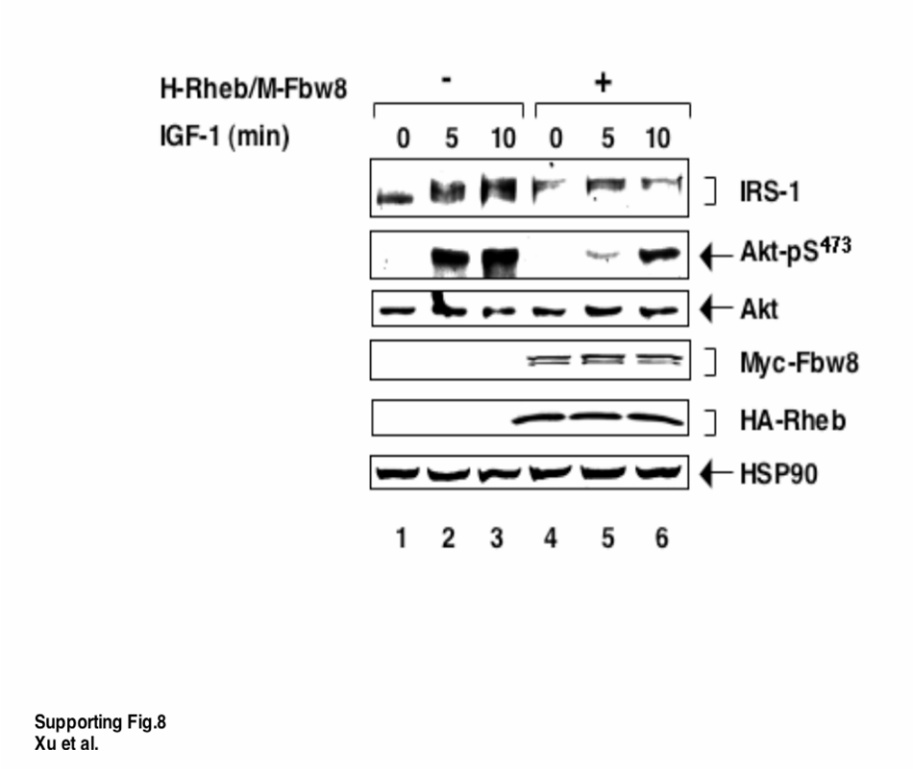

Supporting Fig.8
Xu et al.

Figure S8.

Over-expression of Fbw8 and Rheb delayed Akt activation in response to IGF-1. Given its critical role in mediating the activation of PI3-K/Akt pathway in response to insulin/IGF-1, diminished IRS-1 protein levels are expected to decrease Akt signaling, which can be measured by monitoring its phosphorylation at serine 473 using specific antibodies. MCF-7 cells were co-transfected with (lanes 4-6) or without (lanes 1-3) vectors expressing Myc-Fbw8 and HA-Rheb. At 36h post-transfection, cells were grown without serum and starved for 12h. IGF-1 was added to final concentration of 10nM and the treated cells were incubated for times as indicated. Cell extracts (50μg of protein) were analyzed by immunoblot to monitor the changes in the levels of endogenous IRS-1, Akt phosphorylated at serine 473, and total Akt, as well as to reveal the presence of ectopically expressed Myc-Fbw8 and HA-Rheb. The results revealed that MCF-7 cells, when over-expressing HA-Rheb and Myc-Fbw8 that reduced IRS-1 level by 50% based

on quantitation using Odyssey Infrared Imaging System, exhibited a decreased capacity to produce Ser^{473}-phosphorylated Akt in response to IGF-1 (compare lanes 2 and 3 with lanes 5 and 6). Of note, the total levels of Akt remained unchanged.

Supplemental experimental procedures

Plasmids — The human V5-IRS-1 expression vector, pcDNA3.1-V5-IRS-1, was prepared using the pcDNA3.1/V5-DEST//LR Clonase™ II system (Invitrogen), per manufacturer's instructions, with human IRS-1 coding sequence purchased from Invitrogen (pENTR™221). To construct human IRS-1 point mutants, site-direct mutagenesis was performed with pcDNA3.1-V5-IRS-1 as template, using the QuickChange™ site-directed Mutagenesis Kit (Stratagene) and sets of primers as follows: V5-IRS-1$^{S307A/S312A}$, TCACGCACTGAGGCCATCACCGCCACCGCCCCGG CCAGCATG (5′) and CATGCTGGCCGGGGCGGTGGCGGTGATGGCCTCAGT GCGTGA (3′); V5-IRS-1^{S527A}, CGAAA GAGAACTCACGCGGCAGGCACATCCCCT (5′) and AGGGGATGTGCCTGCCGCGTGAGTTCTCTTTCG (3′); and V5-IRS-1$^{S636A/S639A}$, GACTATATGCCCATGGCCCCCAAGGCCGTATCTGCCCCACAG (5′) CTGTGGG GCAGATACGGCCTTGGGGGCCATGGGCATATAGTC (3′). To prepare V5-IRS-1^{5A}, two sequential mutagenesis reactions were carried out: first using V5-IRS-1$^{S307A/S312A}$ as template with the V5-IRS-1^{S527A} primers, and then using the resulting DNA as template with the V5-IRS-1$^{S636A/S639A}$ primers.

To construct IRS-1 C-terminal truncations, a STOP codon was introduced into the coding sequence at a desired position by mutagenesis with pcDNA3.1-V5-IRS-1 as template, using the QuickChange™ site-directed Mutagenesis Kit (Stratagene) and sets of primers as follow: V5-IRS-1 (1-268), TTCCGCCCT CGCAGCTAGAGCCAGTCC TCGTCC (5′) and GGACGAGGACTGGCTCTAGCTGCGAGGGCGGAA (3′); V5-IRS-1 (1-522), CTGGATAATCG GTTCCGATAGAGAACTCACTCGGCAGGC (5′) and GCCTGCCGAGTG AGTTCTCTATCGGAACCGATTATCCAG (3′); V5-IRS-1 (1-574), GGACACAGGCACTCCTAGTTCGTGCCCACCCGC (5′) GCGGGTGGGCACGAACT

AGGAGTGCCTGTGTCC (3′); and V5-IRS-1 (1-627), GTGCCCAGTGGCCGATAGGG CAGTGGAGACTAT (5′) and ATAGTCTCCACTGCCCTATCGGCCACTGGGCAC (3′).

The GST-Fbw8/Skp1 bacterial co-expression vector, pGEX-4T3/pET-15b-(GST-Fbw8)-(His-Skp1), was created by inserting Fbw8 and Skp1 encoding sequence (Dias *et al*., 2002) into multi-cloning sites on the pGEX-4T3/pET-15b vector, generated as previously described (Wu *et al*., 2000b). All constructs were verified by DNA sequencing.

Antibodies and reagents

The following antibodies were purchased: Skp1, c-Myc, HSP90, Ku-70 (Santa Cruz); ROC1 (Zymed); V5 (Invitrogen); IRS-1 and IRS-1 (pS307) (Upstate); Flag, β-actin, and rapamycin (Sigma); GST (Santa Cruz); and Akt and pAkt (pS473) (Cell Signaling Technology). Anti-CUL7 monoclonal antibody (Mab38) was described previously (Dowell *et al*., 2007). Anti-Fbw8 polyclonal antibody was generated by Covance Research Products, with GST-Fbw8 as antigen that was prepared using a method described previously (Dias *et al*, 2002). The following agents were purchased: human recombinant IGF-1 (Peprotech, Inc); purified human IRS-1 and S6K (Upstate); and E1 (Boston Biochem). PK-Ub and Ubc5c were prepared as described previously (Wu *et al*., 2000a).

Identification of human IRS-1 as an Flag-Fbw8-inetracting protein

To isolate and identify Flag-Fbw8-inetracting proteins, twenty 150mm plates-worth of FF8HEK cells were prepared, extracted, purified and analyzed by mass spectrometry as described previously (Dias *et al*., 2002). Silver stain analysis of Flag-

Fbw8 associated proteins, which were eluted by Flag competing peptides of M2 matrix that had been immuno-adsorbed with extracts from FF8HEK cells. Eluted materials, corresponding to one 150-mm plate-worth of FF8HEK cells, were concentrated and separated by electrophoresis through 4-20% SDS-PAGE. Micro-HPLC/ESI-IT-MS/MS analysis of polypeptides with apparent molecular weight of 150KDa yielded two peptides that matched with those from human IRS-1 as indicated.

***In vitro* binding**

Procedure for preparing glutathione beads bound to the GST-Fbw8/Skp1 complex was described in Supporting Fig. 2A. For *in vitro* binding, purified human IRS-1 (60ng) was incubated with S6K (0.01ng) at 37°C for 30 min in a reaction mixture (20µl) containing 50mM Tris-HCl pH 7.4, 5mM $MgCl_2$, 0.5mM DTT, 1mM ATP, 0.1 mg/ml BSA, 2mM NaF, and 10nM Okadaic acid. The phosphorylation mixture was then mixed with glutathione beads (20µl) containing GST-Fbw8/Skp1. Following incubation at 4°C for 1h, the beads were washed 3 times with buffer containing 10mM Tris-HCl, pH 7.4, 500mM NaCl, 0.5%NP-40, 5mM EDTA, and 5mM EGTA, prior to separation through 6% SDS-PAGE and immunoblot analysis using anti-IRS-1 antibody.

Real-Time PCR

Mouse embryonic fibroblasts were plated at a density of 10^6 per 10-cm-diameter dish. After washing twice with ice-cold PBS, RNA was isolated using the RNeasy kit (Qiagen). Two micrograms of total RNA was applied for reverse transcription by Superscript II reverse transcriptase (Invitrogen). The reaction mixture was diluted 10-fold and an aliquot (3µl) was used for Real-time PCR reaction on a DNA Engine Opticon Real Time

System (MJ Research, Waltham, MA) using the SYBR Green JumpStart Taq ReadyMix kit (Sigma) according to manufacturer's instructions. Primers for mouse IRS-1 (Invitrogen) used for RT-PCR were 5'-GGCAGGGGAGGACTTGAG-3' and 5'-CTGGGTGGAGGGTTGTTG-3'. GAPDH was used as an internal standard.

Cell morphology analysis of CUL7$^{+/+}$ and CUL7$^{-/-}$ MEFs

Cells were fixed with 3.7% PFA (in PBS, RT) and washed with phosphate-buffered saline (PBS) plus 0.1% Triton X-100 and then blocked with 1% BSA in PBS. The cells were then stained with phalloidin Alexa 488 (5µl in 200µl of 1% BSA solution) and washed with PBS, followed by visualization of the actin cytoskeleton and DAPI with the fluorescence microscope. Note the enlarged, flat cell morphology of CUL7 $^{-/-}$ MEFs, particularly pronounced in later passages.

Supplemental References

Arai, T., Kasper, J.S., Skaar, J.R., Ali, S.H., Takahashi, C., and DeCaprio, J.A. (2003). Targeted disruption of p185/Cul7 gene results in abnormal vascular morphogenesis. Proc. Natl. Acad. Sci. U S A. 100(17), 9855-60.

Dias, D. C., Dolios, G., Wang, R., and Pan, Z. Q. (2002). CUL7: A DOC domain-containing cullin selectively binds Skp1.Fbx29 to form an SCF-like complex. Proc. Natl. Acad. Sci. USA 99, 16601-16606.

Dowell, J.D., Tsai, S.C., Dias-Santagata, D.C., Nakajima, H., Wang, Z., Zhu, W., and Field, L.J. (2007). Expression of a mutant p193/CUL7 molecule confers resistance to MG132- and etoposide-induced apoptosis independent of p53 or Parc binding. Biochim Biophys Acta. 1773(3), 358-66.

Wu, K., Fuchs, S.Y., Chen, A., Tan, P., Gomez, C., Ronai, Z., and Pan, Z.-Q. (2000a). The $SCF^{Hos/\beta\text{-}TRCP}$-ROC1 E3 Ubiquitin Ligase Utilizes Two Distinct Domains within CUL1 for Substrate Targeting and Ubiquitin Ligation. Mol. Cell. Biol. *20,* 1382-1393.

Wu, K, Chen, A, and Pan, Z.-Q. (2000b) Conjugation of Nedd8 to CUL1 enhances the ability of the ROC1-CUL1 complex to promote ubiquitin polymerization. *J Biol Chem.* 275, 32317-32324